Steel and Composite Structures, Vol. 13, No. 3 (2012) 225-238
DOI: http://dx.doi.org/10.12989/scs.2012.13.3.225

Experimental study on laterally restrained steel columns with variable I cross sections

Ionel-Mircea Cristutiu*[1], Daniel Luis Nunes[2] and Adrian Ioan Dogariu[2]

[1]*Department of Architecture, PUT, Timisoara-300223, Romania*
[2]*Department of Steel Structure and Structural Mechanics, PUT, Timisoara-300224, Romania*

(Received July 07, 2011, Revised November 23, 2011, Accepted May 17, 2012)

Abstract. Steel structural elements with web-tapered I cross section, are usually made of welded thin plates. Due to the nonrectangular shape of the element, thin web section may be obtained at the maximum cross section height. The buckling strength is directly influenced by lateral restraining, end support and initial imperfections. If no lateral restraints, or when they are not effective enough, the global behaviour of the members is characterized by the lateral torsional mode and interaction with sectional buckling modes may occur. Actual design codes do not provide a practical design approach for this kind of elements. The paper summarizes an experimental study performed by the authors on a relevant number of elements of this type. The purpose of the work was to evaluate the actual behaviour of the web tapered beam-columns when applying different types of lateral restraints and different web thickness.

Keywords: tapered web; experimental tests; finite element; lateral restraints; steel beam-columns; slender elements.

1. Introduction

Steel frame buildings, especially single story ones, are usually made of welded plate elements with tapered web classified as class 3 (elastic) and 4 (slender) according to EN 1993-1-1. The constituent elements are mainly subjected to bending moment and interaction between bending moment and compression. In the case of class 3 sections, when they are restrained against lateral or/and torsional buckling, the interaction between sectional plastic buckling and overall buckling of the members in compression and/or in bending is possible. When class 4 (slender) sections are used, which generally is the case of the rafter at the maximum height of the tapered web, the sectional buckling (e.g., local buckling of walls or distortion) may occur in the elastic domain. If no lateral restrains, or when they are not effective enough, the lateral torsional mode could characterize the global behaviour of the frame members or interaction with sectional bucking modes may occur as well.

Tapering of the elements is made in accordance with internal force distribution under gravitational loads, which are predominant in the design of these types of structures.

Structural stability is the fundamental safety criterion for buildings, both during their functioning period and construction lifetime. The current European standard EN 1993-1-1, contains numerical

* Corresponding author, Ph.D., E-mail: mircea.cristutiu@arh.upt.ro

procedures for buckling verification of steel structural elements, which differ from the traditional simplified procedures. The latter only covered regular geometrical shapes, simple load cases and classical supports (rigid or pinned). Nowadays advanced numerical computer-aided analyses can be performed which allow the investigation of complex structures by using European provisions. This allows one to use a greater number of factors that affect the structure in what concerns their stability: geometrical imperfections, material nonlinearities, production residual stresses, element lateral restraining, and real element boundary conditions. Although, the actual standards are more complex than the previous ones, interaction formulas for the strength and buckling verification of individual elements for different type of load (e.g., tension, compression, bending, shear, twisting, and combination between them) are provided only for uniform members. There are some provisions that could be applied for the design of tapered members, namely "the general method". However its application involves advanced structural analysis (e.g., linear eigen buckling and elasto-plastic analysis).

Even though many researchers have performed investigation on the uniform elements subjected to bending moment and axial compression force (Taras 2008, Szalai 2009, Farshi 2009), information regarding the out-of-plane behaviour of tapered elements is still limited. The ultimate capacity for tapered steel plate girders subjected to shear was determined by Shanmugam (2007) and the one for axially loaded thin-walled tapered columns with doubly symmetric sections by Salem (2009). Shanmugam (2007) experimentally determined the ultimate behaviour of tapered steel plate girders and concluded that the shear capacity of the girder is 5% less than in the case of the prismatic one, if the inclined flange is tensioned. Whilst inclined flange is subjected to compression, the ultimate load of the tapered girder increases by more than 5% compared to that of straight girders.

The aim of the present paper is to analyze the behaviour of tapered column elements subjected to bending moment and axial compressive force when different type of lateral restraints are applied. Results of an experimental program carried out at the "Politehnica" University of Timisoara, Romania in the Laboratory of Steel Structures will also be presented. A three dimensional finite model will be presented as well and the results will be compared with the experimental ones.

2. Experimental program

2.1 Test specimens

A simple pitched-roof portal frame, as the one in Fig. 1, was designed at first in order to define realistic specimen configurations. The main geometric dimensions of the frame were: 12 m span, 6 m bay, 4 m height and a pitch roof angle $\alpha = 8^0$. Common load cases according to EN1991 provisions were considered i.e., characteristic dead load of roof cladding $g_k = 0.7$ kN/m^2; characteristic snow load $s_k = 2.0$ kN/m^2. The load combination considered for the ultimate limit state was $1.35g_k+1.5s_k$, and for the serviceability limit state was $1.0g_k+1.0s_k$. The steel frame was analysed and designed according to the current EN 1993-1-1 provisions. The frames were considered pinned at the foundation level, while the rafter-to-column connection was considered fully rigid. The column specimens were extracted from the resulting frame and their global geometrical dimensions are presented in Fig. 2. In order to analyse the influence for the web thickness on the column behaviour, two different values (i.e., 6 and 8 mm) were considered.

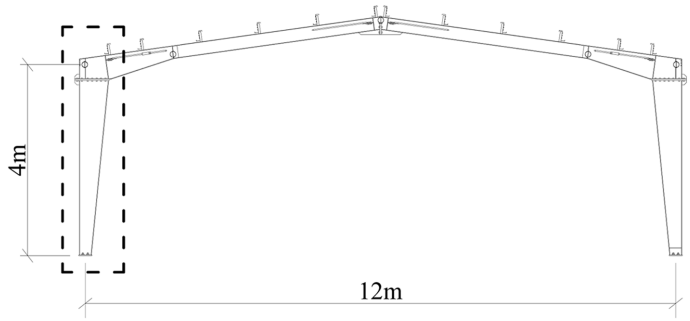

Fig. 1 Reference frame

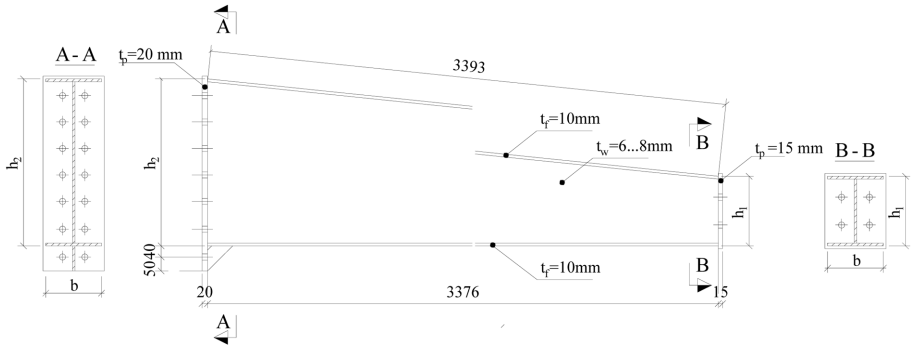

Fig. 2 Specimen typology (dimensions are in mm)

Table 1 Specimen main dimension

Specimen	L [mm]	h_1 [mm]	h_2 [mm]	b	t_f	t_w
C1_8	3376	250	600	200	10	8
C2_6	3376	250	600	200	10	6

The cross section dimensions of the two types of specimens and their codification are presented in Table 1.

Fillet weld of 5 mm was provided between the flange and the web of the specimen, while effective full penetration T-butt welds were considered for the connection between flange and end plates. The outer flange was kept horizontally, whilst the second one was inclined following the shape of the tapered web. The connection at the left hand side (top in case of frames) of the specimen was assumed to be rigid, thus a 20 mm thick extended end plate was provided accordingly. The bolts in the connection were of 20 mm in diameter with 12.9 steel grades (yield limit f_y = 1080 N/mm^2). The opposite side of the specimen was considered pinned with a 15 mm flush end plate. The bolts were of 20 mm in diameter with 8.8 steel grades (yield limit f_y = 640 N/mm^2). Taking into account the measured tensile strength, the web cross section classes for the two specimens were evaluated and are illustrated in Fig. 3. The flanges are of Class 3 (elastic) for both cases.

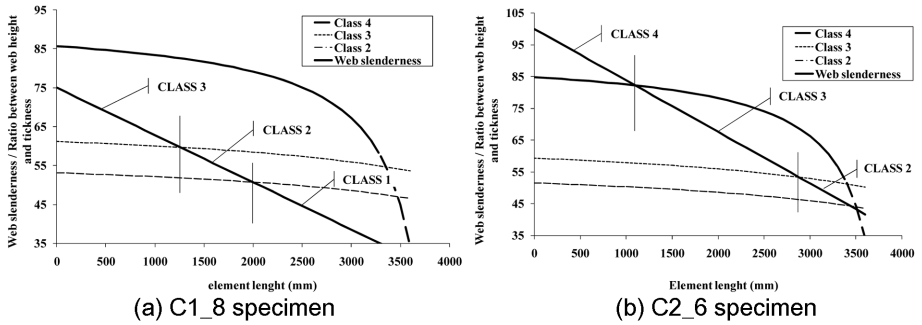

Fig. 3 Cross section class (web slenderness) for the two considered specimens

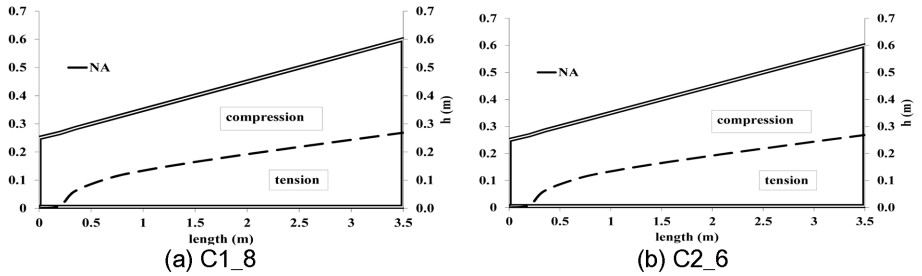

Fig. 4 Distribution of normal stresses for design values of the internal forces (N_{Ed}, M_{Ed})

Fig. 4 shows the normal stress distribution, on the selected specimens, resulting from the combined action of axial compression and bending moment. The design values of internal forces taken into consideration in the evaluation of the normal stress were: N_{Ed} = 143 kN and M_{Ed} = 270 kNm. These values were obtained from the ultimate limit state combination.

2.2 Material properties

Tensile tests were performed on coupons extracted from the same plate as the one used for the fabrication of the tests specimen (Fig. 5). For each thickness three coupons were tested. The tensile test

Fig. 5 Tested coupons after tensile test (t = 6, 8, 20, 15, 10 mm, starting from bottom left counterclockwise)

Table 2 Measured values for tensile test

Coupon	t mm	f_y Mpa	f_u Mpa	f_u/f_y
P1-6-1	6	319	491	1.540
P2-6-2	6	321	502	1.562
P3-6-3	6	317	488	1.540
P4-8-1	8	407	520	1.276
P5-8-2	8	410	522	1.272
P6-8-3	8	413	514	1.245
P7-10-1	10	271	393	1.451
P8-10-2	10	265	406	1.531
P9-10-3	10	266	403	1.515
P10-15-1	15	296	425	1.435
P11-15-2	15	298	418	1.402
P12-15-3	15	294	417	1.419
P13-20-1	20	426	564	1.325
P14-20-2	20	426	528	1.239
P15-20-3	20	428	529	1.235

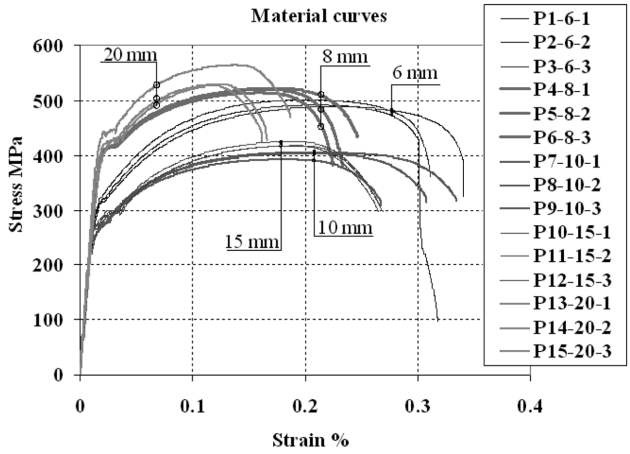

was carried out using a UTS RSA 250 kN-universal test machine. The obtained results are presented in Table 2, indicating the resulted yield strength (f_y) and ultimate tensile strength (f_u) for each specimen. For the purpose of this work, measured values will be used from this point forward.

2.3 Test setup and instrumentation

Three specimens of each configuration were tested, finally resulting in a number of six experimental tests (Table 3). The difference between the tests, for each specimen, was the provided type of lateral restraints. Three of the specimens had 8 mm tapered web (C1-8) and the other three were designed with 6 mm tapered web (C2-6). The types of lateral restraints considered for each specimen configuration were (Fig. 6): (NR) – no restraints, (LR) – lateral restraints; and (TR) – torsional restraints respectively. Lateral restraints (LR) were provided by thin walled cold formed "Zed" purlins (Z150/1.5 mm), while in the case of torsional restraints (TR) supplementary L50×50×5 fly braces were provided at the compressed flange.

Table 3 Specimens and type of lateral restraints

Specimen	L [mm]	h_1 [mm]	h_2 [mm]	b	t_f	t_w	Restraint
C1_8_NR	3376	250	600	200	10	8	No Restraints
C1_8_LR	3376	250	600	200	10	8	Lateral Restraints
C1_8_TR	3376	250	600	200	10	8	Torsional Restraints
C2_6_NR	3376	250	600	200	10	6	No Restraints
C2_6_LR	3376	250	600	200	10	6	Lateral Restraints
C2_6_TR	3376	250	600	200	10	6	Torsional Restraints

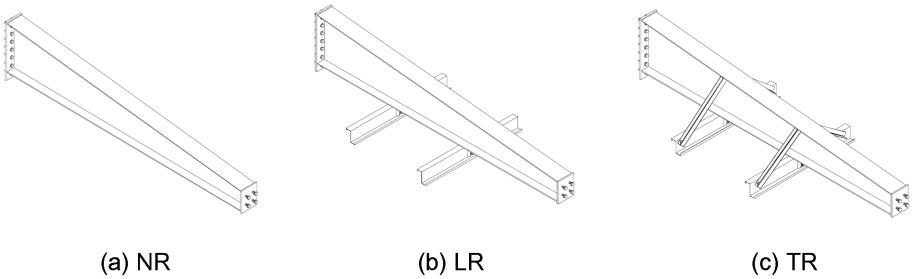

Fig. 6 Lateral restraints considered in experimental test

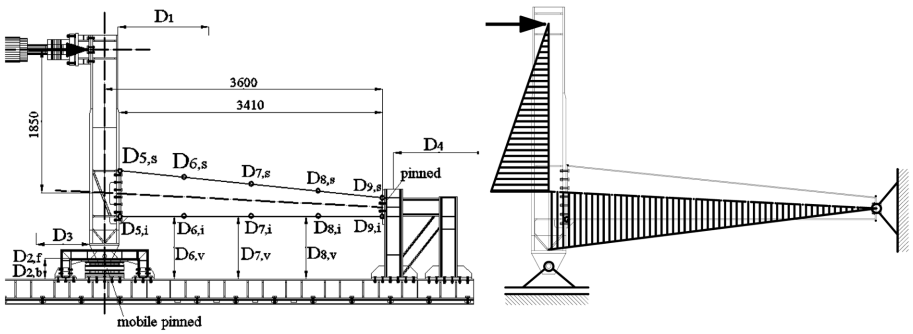

Fig. 7 Testing setup and loading scheme

The applied static scheme is a simple one, i.e. pinned connection at the right end of the column, and a roller at the bottom of the vertical element. The latter was designed stiff enough, so as not to suffer major deformations during testing. A horizontal force was applied at the end of the vertical element.

The applied load and boundary conditions were designed in such a way as to load the specimen by a combination of axial compressive load and bending moment (Fig. 7). The testing set-up was designed in such a way as to maintain the vertical element in the elastic range and to replace only the specimen for each test. The load was applied through a Quiri hydraulic jack, with a maximum capacity of 1000 kN.

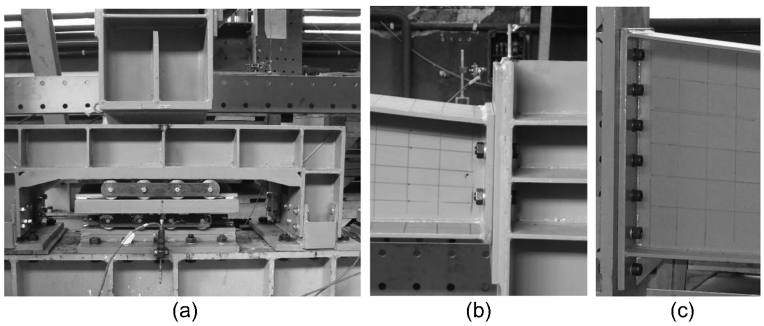

Fig. 8 Boundary conditions for the test setup: (a) roller, (b) pinned column base, (c) rigid column connection

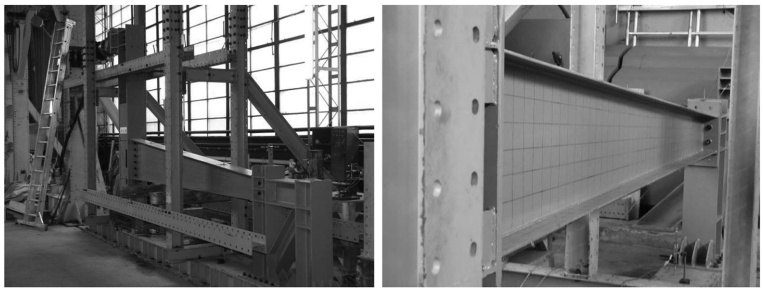

Fig. 9 Testing setup and specimen position

The bottom roller was designed in such a way as to allow horizontal displacement and to prevent vertical displacement both upwards and downwards. In order to transfer the bending moment directly from the vertical element onto the tested column, it was very important that roller worked properly (Fig. 8). Apart from allowing free horizontal displacement, the simple support also prevented the appearance of a horizontal reaction force that would lead to the change of the bending moment diagram. The connection of the tested column was considered rigid at the left end and pinned at the right one. The fixed connection was designed with extended end plate bolted configuration, while the pinned one using a flush end plate.

The tests have been conducted in displacement control procedure. The load was applied quasi-statically with a displacement velocity of 3.33 mm/min. The overall view of the test setup is presented in Fig. 9.

Side guides were applied at the top of the vertical element to avoid out of plane displacement and twisting of the loading frame due to inherent imperfection. The in plane and out of plane displacement were monitored during tests using 18 Novotechnic displacement transducers (Fig. 7). Some of them (e.g., D1, D3...D9) measured absolute displacement of the indicated points with regard to points independent from the testing frame. Others (e.g., D2f, b) measured the relative displacement between points located on the tested frame.

3. Finite element modelling

It is generally known that experimental tests are both time and labour consuming. However, if the boundary conditions and applied forces are not adequately provided, the final results of the experimental test could be altered significantly. The finite element modelling is a powerful tool that would be an alternative for the experimental test regarding the analysis of the behaviour and in establishing the ultimate capacity of steel structural elements. For the purpose of the present work some finite element models were built. Numerical simulations were performed in accordance with EN 1993-1-5 Annex C that gives guidance for the use of FE-methods in order to evaluate the ultimate capacity. The commercial finite element package Abaqus v6.5-1 has been used. This software has proven its reliability in many benchmark studies and was considered suitable for the current task.

A finite element model was built using shell and solid elements following the exact nominal geometrical dimensions of the tested specimens. Shell elements were used mainly for the modelling of the straight parts, whilst solid elements were considered for the modelling of the connections (Fig. 10). Consequently a three dimensional model was obtained whereon real test boundary conditions were applied. Surface-to-surface contact was provided between the end plate of the specimen and the flange

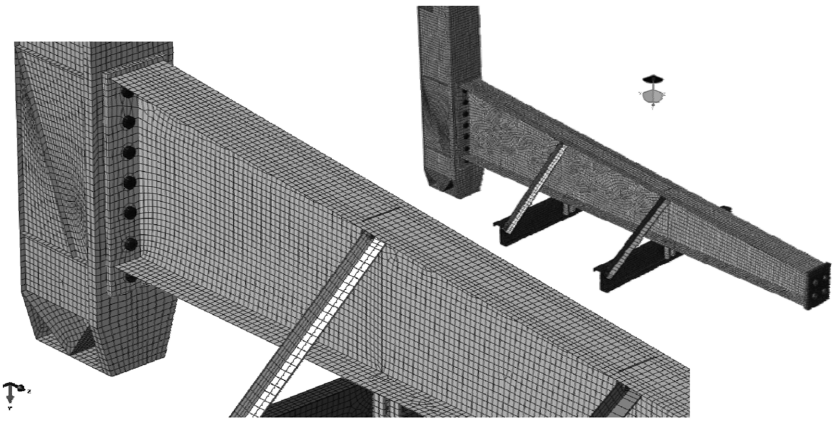

Fig. 10 Finite element models

of the vertical element, as well as between the bolts and the connected parts.

Using this complex model geometrical and material nonlinear analysis were performed on the perfect element (i.e., GMNA). A four and three node, quadrilateral and triangular shape of linear geometric order, S4R, respective S3, finite elements were used.

Both geometrically and materially nonlinear behaviour were considered, together with the equivalent global bow geometric imperfection, to determine elastic-plastic resistance in ULS, using GMNIA. Imperfections were applied according to EN1993-1-1 provisions, i.e., out of plane initial bow imperfection with the amplitude of 1/150 from the length of the tested specimen, corresponding to a plastic analysis of a welded I-section element (buckling curve c about minor axis z-z). The considered equivalent imperfections take account for residual stresses and geometrical imperfections such as lack of verticality, lack of straightness, lack of flatness, lack of fit and any minor eccentricities present in the joints of the unloaded structure. Most of the standard provisions do not consider torsional imperfection (except AS4100) due to its small influence, hence no such imperfection were introduced in the analysys. Even if in some sections of the member (i.e., tapered section), class 4 of cross-section was obtained, the local sectional imperfection was not considered individually, this being accounted in the considered equivalent imperfections.

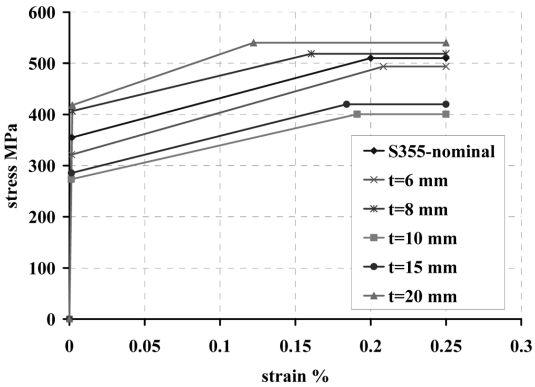

Fig. 11 Material behaviour curve – FEM analysis

A high accuracy was expected so the real experimental measured material behaviour parameters (i.e., yield limit f_y and ultimate strength f_u) have been used. The material behaviour was modelled by an elastic-plastic with linear strain hardening model (Fig. 11).

4. Experimental and finite element results

The results obtained from experimental tests and finite element modelling are presented herein in the forms of tables and graphs. The first results recorded during the tests have been in terms of forces (F) and displacements (d). These results were converted thereafter in terms of bending moment (M) and rotation (ϕ) and finally the (M-ϕ) curve was built. The moment rotation curve, plot in Fig. 12 and Fig. 14, shows the behaviour from the elastic to the ultimate capacity of the tapered columns laterally restrained or not.

The reduced moment at the top of the column (left side of the specimen) was computed using Eq. (1) whilst the rotation of the specimen at the front of the vertical element was computed using Eq. (2)

$$M_{red,EX} = (F \cdot L) \cdot \frac{L_{ca}}{L_{cn}} \tag{1}$$

where: $M_{red,EX}$ = reduced bending moment at the column top; F = applied horizontal force; L_r = level arm of the applied force, distance between point of applied force and intersection of neutral axis of vertical column and tapered column (L_r = 1.85 m); L_{cn} = nominal length of the column (3.6 m); L_{ca} = actual length of the column (3.41) (see Fig. 7).

Table 4 Summarized bending moment capacities, FEM- experimental

Specimen	M_{FEM} [kNm]	M_{EXP} [kNm]
C1_8_NR	474.51	488.75
C1_8_LR	491.91	485.79
C1_8_TR	527.09	534.44
C2_6_NR	388.04	395.75
C2_6_LR	395.93	382.43
C2_6_TR	394.82	386.19

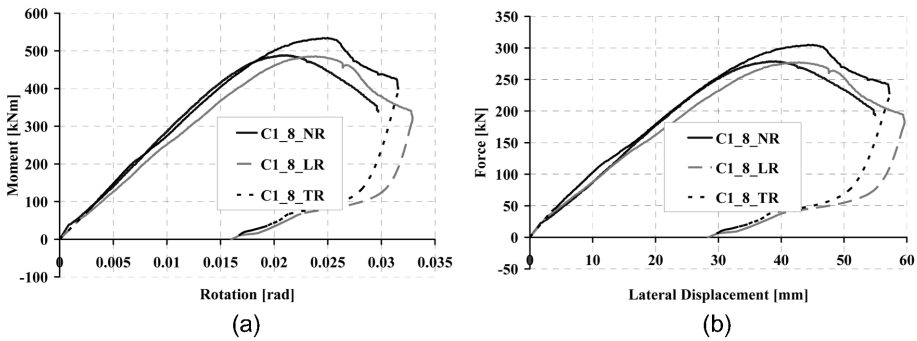

(a) (b)

Fig. 12 C1-8-Behavior curves: (a) Moment-rotation curve, (b) Force lateral displacement curve

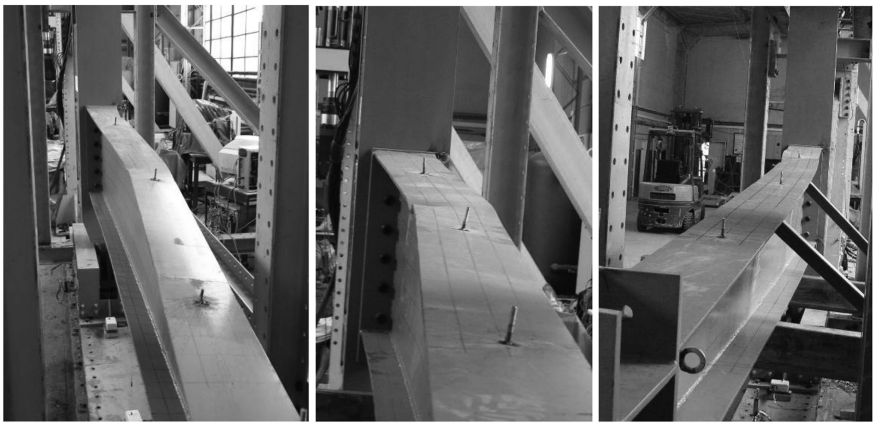

Fig. 13 Failure of the specimen with 8 mm tapered web

$$\phi = atan\left(\frac{D_1}{L_r}\right) \tag{2}$$

where: ϕ = rotation of the specimen with respect to it initial position; D_1 = measured displacement; L_r = level arm of the applied force (L_r = 1.85 m).

The experimental bending moment within the specimen and the corresponding values obtained from the finite element analysis are summarized in Table 4. In Table 4 M_{FEM} refers to the finite element results while M_{EXP} to the experimental tests. The moment-rotation curve and force-lateral displacement curve for the C1-8 series of test are depicted in Fig. 12(a), 12(b). The ones for the series of C2-6 are described in Fig. 14(a), 14(b).

Failures of the specimen, recorded during experimental tests, for different type of lateral restraints, are illustrated in Fig. 13 for C1-8 series specimens. The one recorded for C2-6 specimens are illustrated in Fig. 15. It is important to note that for the case of C1-8 series, the failure is influenced by the type of the lateral restraints. Although the same influence of the lateral restraints should have been recorded in case of C2-6 series, the obtained results did not confirm it. Regarding the latter the lateral restraints had a reduced influence both from behaviour point of view and failure mode (i.e., distortion of the compressed flange coupled with a local buckling of the column).

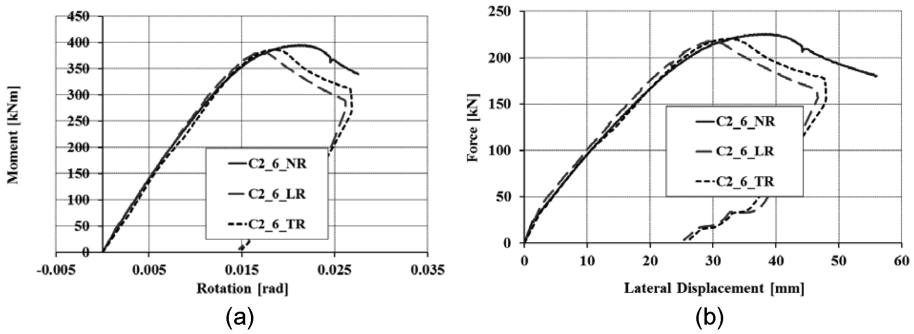

Fig. 14 C2-6-Behavior curves: (a) Moment-rotation curve, (b) Force lateral displacement curve

Fig. 15 Failure of the specimen with 6 mm tapered web

The failure modes of the C1-8 series of tests can be described as: C1_8_NR – at first, overall lateral-torsional buckling of the column was observed, followed by distortion of the compressed flange and finally the specimen failing by sectional plastic buckling; C1_8_LR – at first overall lateral-torsional buckling of the column was observed, followed by distortion of the compressed flange an finally the specimen failing by sectional plastic buckling; C1_8_TR – started with distortion of the compressed flange and was followed by a slight overall torsional buckling ending in sectional plastic buckling.

The failure modes of the C2-6 series of testes can be described as follows: C2_6_NR – started with distortion of the compressed flange, followed by isolated sectional buckling and slight overall lateral-torsional buckling of the column; C2_6_LR – starting with distortion of the compressed flange, followed by isolated sectional buckling and slight overall lateral-torsional buckling of the column; C2_6_TR

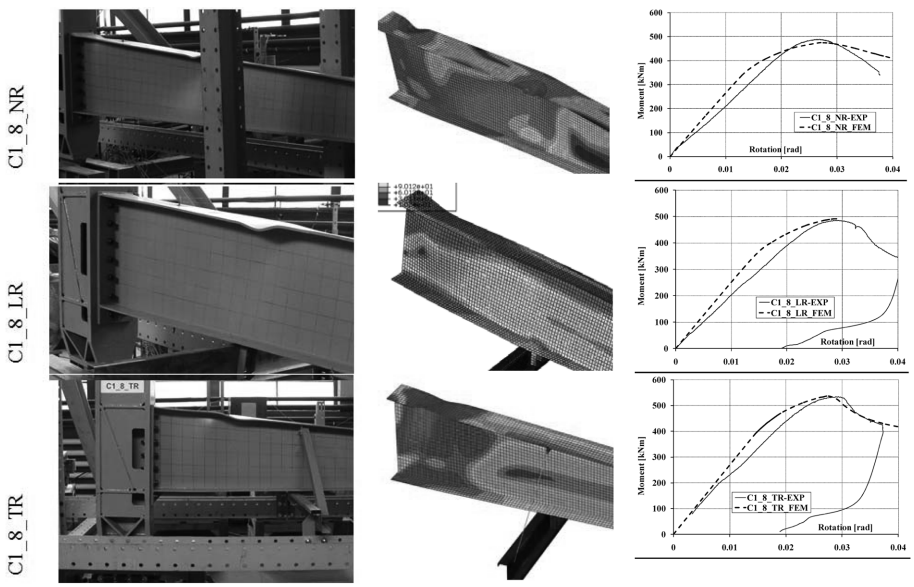

Fig. 16 FEM vs experimental test – C1_8 series

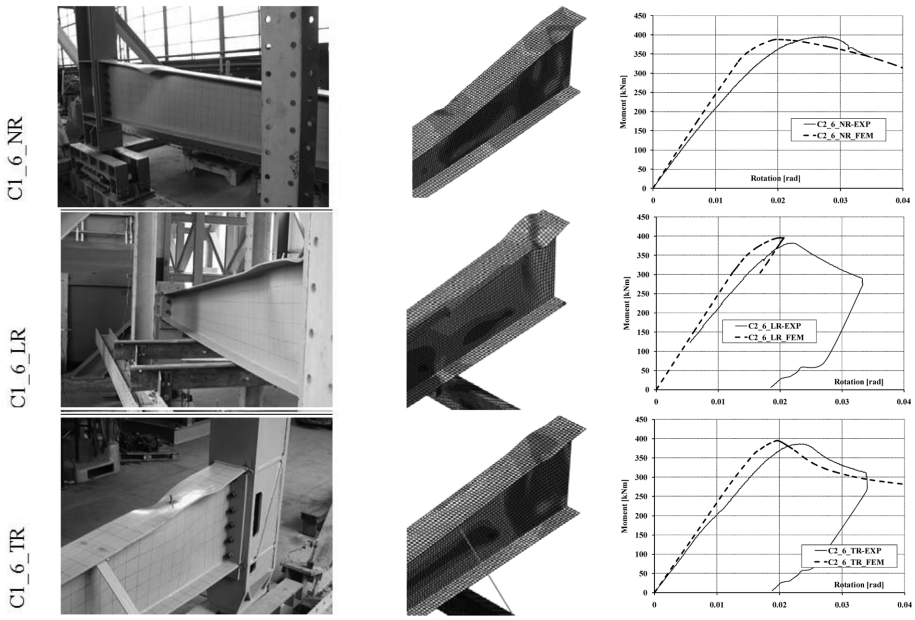

Fig. 17 FEM vs experimental test – C2_6 series

starting with distortion of the compressed flange, followed by isolated sectional buckling and slight overall lateral-torsional buckling of the column. The isolated sectional buckling for this series of tests prevails over the global out of plane buckling. For this type of specimen series, the failure is almost the same regardless of the type of lateral restraints.

Von Misses stress distribution at the levels of flange and web are given to emphasize how the yielding zones develop according to increased load. Moment-rotation curves resulting from the tests are compared with those obtained from the finite element analysis as to verify both the accuracy of the finite element model and experimental test.

Views at the ultimate capacity loading of the considered specimens are shown along with the corresponding finite element predictions (Figs. 16 and 17). Generally a good arrangement can be observed between the deflected web parts and those obtained from finite element analysis. Similar observations could also be made with regards to deformations in flanges.

5. Conclusions

Both the experimental and finite element study of the behaviour and load carrying capacity of tapered web beam-columns have been depicted in the present work. A number of six specimens with different web thicknesses and lateral restraints were tested. For this case the web slenderness is quite significant, while the global slenderness is rather low (ranging from 0.26-0.74) and hence the failure is dominated mainly by local modes.

Based on the results presented within the article, it can be concluded that the finite element modelling is reliable in predicting the ultimate capacity of the elements with tapered web under both compression and bending with sufficient accuracy.

The failure mechanism for the selected specimen series varies in function of the web thickness and lateral restraints (i.e., global out of plane buckling governs in case of 8 mm thickness specimen, whilst distortion of the compressed flange and local web buckling for the case of 6 mm thickness web). The ultimate capacity is significantly influenced by the width/thickness ratio of the web (i.e., 8 mm to 6 mm web thickness). A reduction of 20% was recorded for unrestrained element. However this difference increases with up to 38% for the case of torsional restrained element.

From the experimental results one can conclude that the restraining contribution from the purlins alone is reduced (their effect is mall) for both specimen series. This might be explained by the small influence of the axial compressive force on the behaviour of beam-column elements with variable cross sections. The cross section twists rather than buckles laterally, due to the distribution of the normal stresses on the height of the cross section. The ultimate capacity can be improved by applying a supplementary restraining at the compressed flange, but this is only possible with the use of thicker web element (i.e., t = 8 mm).

It was also observed that both the lateral and torsional restraints played an insignificant role in the case of the slenderer web models. This might be explained by the major influence of plastic sectional buckling, even though slight lateral out of plane buckling was also observed.

Acknowledgements

The authors gratefully acknowledge the financial support of "National University Research Council - NURC-CNCSIS-Romania through the national research grant PN-II-RU-TE-2010-1/38.

References

Abaqus, v.6.5.1, Dassault Systems/Simulia, Providence, RI, USA; 2008.

AS 4100-1998. Australian Standard: Steel Structures. Australian Building Codes Board.

Cristutiu, I. M. and Muntean, N. (2010), "Erection and manufacturing imperfection influence on steel frame behaviour", *Proceedings of International workshop "Global and regional environmental protection (GLOREP 2010),* Timisoara, November.

Consteel v.6.0 user manual (2011), Developed by Consteel Ltd. Budapest.

Davies, J. M. (1990), "In-plane stability in portal frames", *The Structural Engineer*, **68**(8), 141-147.

Dubina, D. and Cristutiu, I. M. (2005), "Buckling strength of pitched roof portal frames of Class 3 and 4 tapered members" *Proceedings of EUROSTEEL 2005-4th European Conference on Steel and Composite Structures*, Maastricht, June.

Duthinh, D. and Fritz, W. P. (2007), "Safety Evaluation of Low-Rise Steel Structures under Wind Loads by Nonlinear Database-Assisted Technique". *J. Struct. Eng. ASCE*, 0733-9445(2007)133: **4**(587), 587-594.

EN 1991-1-1 Eurocode 1. (2002), "Actions on structures - Part 1-1: General actions - Densities, self-weight, imposed loads for buildings", CEN-CEN-Brussels, Belgium, 2002.

EN 1991-1-1 Eurocode 1. (2003), "Eurocode 1 - Actions on structures - Part 1-3: General actions -Snow loads", CEN-CEN-Brussels, Belgium, 2003.

EN 1993-1-1 Eurocode 3. (2005), "Design of steel structures Part 1.1: General rules and rules for buildings", CEN-CEN-Brussels, Belgium, 2005.

EN 1993-1-5 Eurocode 3. (2003), "Design of steel structures Part 1.5: Plated structural elements", CEN-CEN-Brussels, Belgium, 2003.

Farshi, B. and Kooshesh, F. (2009), "Buckling Analysis of structural steel frames with inelastic effects according to codes" *J. Constr. Steel Res.,* **65**(2009), 2078-2085.

Goncalves, R. and Camotim, D. (2005), "On the incorporation of the equivalent member imperfections in the in-plane design of steel frames", *J. Constr. Steel Res.,* **61**(2005), 1226-1240.
Jimenez, G. A. and Galambos, T. V. (2008), "In plane and out of plane behaviour of web tapered beam-columns" *Proceedings of EM08- Inaugural International Conference of the Engineering Mechanics Institute*, Minnesota, May.
Kala, Z. (2011), "Sensitivity Analysis of Steel Plane Frames with Initial Imperfections", *Eng. Struct.*, **33**(8), 2342-2349.
Kala, Z. (2011), "Sensitivity Analysis of Stability Problems of Steel Plane Frames", *Thin-Walled Structures*, **49**(5), 645-651.
Nagy, Zs. et al. (2010) "Case study: The supporting steel structure of the ice rink – city of Tg. Mureş, Romania", *Proceedings of the 1-st International Conference on Structures & Architecture – ICSA2010*, Guimaraes, July.
Nagy, Zs. and Cristuþiu, I. M. (2010). "Advanced nonlinear investiga-tions of a 50 m span frame case study: The steel structure of the ice rink, city of Târgu Mureş, Romania". *Proceedings of Stability and Ductility of Steel Structures, SDSS-2010*, Rio de Janeiro, September.
Raftoyiannis, I. G. and Ermopoulos, J. C. (2005), "Stability of tapered and stepped steel columns with initial imperfections" *Eng. Struct.,* **27**(2005), 1248-1257.
Salem, A. H. et al. (2009). "Ultimate capacity of axially loaded thin-walled tapered column with doubly symmetric sections". *Thin Walled Structures,* **47**(2009), 931-941.
Simões da Silva, L., Rebelo, C. and Marques, L. (2009), "Application of the general method for the evaluation of the stability resistance of non-uniform members," *Proceedings of the Sixth International Conference on Advances in Steel Structures - ICASS 09*, Hong Kong, China, December.
Shanmugam, N. E. and Min, H. (2007), "Ultimate load behaviour of tapered steel plate girders", *Steel. Compos. Struct.,* **7**(6), 469-486.
Szalai, J. and Papp, F. (2009), "On the probabilistic evaluation of the stability resistance of steel columns and beams", *J. Constr. Steel Res.,* **65**(2009), 569-577.
Taras, A. and Greiner, R. (2008), "Torsional and flexural torsional buckling - A study on laterally restrained I-sections", *J. Constr. Steel Res.,* **64**(2008)*7-8*, S. 725-731.
Taras, A. and Greiner, R. (2008), "Development of consistent buckling curves for torsional and lateral-torsional buckling", *Steel Constr.,* **1**(2008)1, S. 42-50.

CC